Proceedings of the 19th International Conference on Automation & Computing, Brunel University, London, UK, 13-14 September 2013

Fault Detection and Isolation for Open-loop Chylla-Haase Polymerization Reactor

Abdelkarim M. Ertiame[1], Dingli Yu[2], Feng Yu[3], J. B. Gomm[4]
[1, 2, 4] Control System Research Group, School of Engineering
Liverpool John Moores University, Byrom Street,
Liverpool, L3 3AF, United Kingdom
[1]A.M.Ertiame@2011.ljmu.ac.uk
[3] School of electronic Information, Changchun Architecture &Civil Engineering College
Changchun, Jilin Province, China

***Abstract*—Fault detection and fault diagnosis have become increasingly important for improvement of the reliability, safety and efficiency of many technical processes. In this research, a new robust fault detection and isolation (FDI) scheme is developed for open-loop Chylla-Haase polymerization reactor. This reactor has been widely used as an industrial Benchmark. The independent Radial Basis Function (RBF) Neural Network (RBFNN) is employed here for on-line diagnosis of faults on the actuator, sensors, and reactor components when the system is subjected to system uncertainties and disturbances. Two different techniques to employ RBF neural networks are investigated. Firstly, an independent neural network is used to model the reactor dynamics and generate residuals. Secondly, an additional RBF neural network is developed as a classifier to isolate faults from the generated residuals. Three sensor faults and one actuator fault are simulated on the Chylla-Haase reactor. Moreover, many practical disturbances and system uncertainties, such as monomer feed rate, fouling factor, impurity factor, ambient temperature and measurement noise are modelled. The simulation results are presented to illustrate the effectiveness and robustness of the proposed method.**

***Keywords*— Robust fault detection; independent RBF model; RBF neural networks; open-loop Chylla-Haase reactor.**

I. INTRODUCTION

In recent years, the task of monitoring complex nonlinear processes has been intensively studied. Fault detection and isolation (FDI) techniques have attracted much interest due to the increasing demand for good performance and higher standards of safety and reliability of technical plants for improving the supervision and monitoring as part of the overall control of processes[1]. FDI has become a critical issue in the operation of high-performance chemical plants, nuclear plants, airplanes, ships, submarines, and space vehicles, etc. [2]. In the chemical industry, faults can occur due to sensor failures, equipment failures or changes in process parameters. Occurrence of a fault may cause process performance degradation, or in the worst cases, may cause disastrous accidents. However, FDI can help avoid all these major consequences [3 and 11].

Due to serve nonlinearity and time varying feature of the reactor dynamics, the observer methods, parity space methods, and other first-principle model based methods cannot be successfully applied for FDI of the Chylla-Haase reactor.

Many research works have been carried out to study NNs for FDI. Yu et al [4] studied sensor fault diagnosis in chemical process via RBF neural networks; a semi-independent NN was used for sensor fault diagnosis. Moreover, the thins-plate-spline function was used for the neural model and the Gaussian function was used for the neural classifier. Another study was conducted by Gomm and Yu [5] that introduced the selection of radial basis function (RBF) network centres with recursive orthogonal least squares training. Frank and Seliger [6] studied fuzzy logic and neural network applications for fault diagnosis. Their paper introduced fuzzy logic for residual evaluation, a dependent neural network for residual generation, and a neural network for residual evaluation by using another dependent neural network for generating residuals. All those authors used dependent and semi-dependent mode of NN for FDI. As the residual of these methods is affected by the plant output, the residual is made insensitive to the faults. Although a partial dependent mode is used to enhance the residual to fault sensitivity, the fault detect threshold is still high such that fault with small amplitude cannot be detected [9, 10, and 11].

In this research, a new robust FDI scheme is developed for open-loop Chylla-Haase polymerization reactor. The independent Radial Basis Function Neural Network (RBFNN) is employed here for on-line diagnosis of faults on the actuator, sensors, and reactor components when the system is subjected to system uncertainties and disturbances. The independent neural network mode is developed to generate enhanced residuals for diagnosing faults in the reactor. Then, a second neural network is developed as a classifier to isolate these faults. The basis Gaussian function is used for the neural network model, and for the neural network classifier. The K-means clustering algorithm is used to choose the centres of the RBF networks, and a p-nearest-neighbours algorithm is used to choose the widths. Moreover, a recursive least squares (RLS) algorithm is used to update the weights.

II. THE CHYLLA-HAASE BENCHMARK REACTOR

Batch and semi-batch reactors have been widely used in the chemical industry. In this research, a semi-batch polymerization reactor benchmark is considered which is described by Chylla and Haase [8] and used as a benchmark for process control applications. The schematic diagram of the semi-batch polymerization reactor is shown in Fig.1 [8]. It consists of a stirred tank reactor with cooling jacket and a coolant recirculation. The reactor temperature is controlled by manipulating the temperature of the coolant, which is recirculated through the cooling jacket of the reactor. The heat released through the reaction must be removed by circulating cold water through the jacket, where both hot and cold jacket streams are available. When the jacket temperature controller output is between 0 and 50%, the valve is opened and cold water is inserted, and when the jacket controller output is between 50 and 100%, the valve is opened and steam is inserted [8].

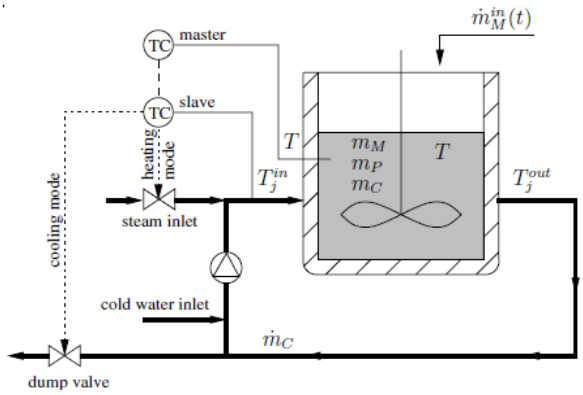

Figure 1. Chylla-Haase reactor schematic.

A. Polymerization Reactor Model

The mathematical model of the Chylla-Haase reactor is described by a set of five ordinary differential equations (ODE) which come from material and heat balances inside the reactor:

$$\frac{dm_M}{d_t} = \dot{m}_M in(t) + \frac{Q_{rea}}{\Delta H} \tag{1}$$

$$\frac{dm_p}{d_t} = -\frac{Q_{rea}}{\Delta H} \tag{2}$$

$$\frac{dT}{dt} = \frac{1}{\Sigma_j m_i C_{p,i}}[\dot{m}_{Min}(t) C_{p,m}(T_{amb} - T)\, UA(T - T_j) - (UA)_{loss}(T - T_{amb}) + Q_{rea}] \tag{3}$$

$$\frac{dT_{jout}}{dt} = \frac{1}{m_C C_{p,C}}[\dot{m}_C C_{p,C}(T_{jin}(t-\theta_1) - T_{jout}) + UA(T - T_j)] \tag{4}$$

$$\frac{dT_{jin}}{dt} = \frac{dT_{jout}(t-\theta_2)}{dt} + \frac{T_{jout}(t-\theta_2) - T_{jin}}{\tau_p} + \frac{K_p(c)}{\tau_p} \tag{5}$$

The reactor model includes the material balances (1) and (2) for the monomer mass $mM(t)$ and the polymer mass $mP(t)$, the energy balance (3) with the reactor temperature $T(t)$, plus the energy balances (4) and (5) of the cooling jacket and the recirculation loop with the outlet and inlet temperatures $T_j^{in}(t)$ and $T_j^{out}(t)$ of the coolant.

The heating/cooling function $K_p(c)$ is influenced by an equal-percentage valve with valve position $c(t)$ and the following split-range valve characteristic:

$$K_p(c) = \begin{cases} 0.8 * 30^{\frac{-c}{50}}(T_{inlet} - T_{jin}(t)) & c < 50\% \\ 0 & c = 50\% \\ 0.15 * 30^{\frac{c}{50-2}}(T_{steam} - T_{jin}(t)) & c > 50\% \end{cases} \tag{6}$$

For $c < 50\%$, ice water with inlet temperature T_{inlet} is inserted in the cooling jacket, whereas a valve position $c > 50\%$ leads to a heating of the coolant by injecting steam with temperature T_{steam} into the recirculating water steam.

III. RESIDUAL GENERATION WITH RBF MODEL

A. *Independent Model of RBF Modelling*

Using RBFNN for modelling, a non-linear dynamic system can be modelled in two modes: a dependent mode and an independent mode. The first model referred to is a dependent mode, since the past system output is used as network input. Thus, the model is dependent on the system output and cannot operate independently from the system. In the independent mode, the past model output is used as network input. Therefore, the model is not dependent on the system output and can operate independently from the system. The independent model has an advantage in that the model can be used to simulate the system to obtain long-range prediction. In contrast, the dependent model performs as one-step-ahead predication.

The RBF network performs here as nonlinear mapping, and is used because of its advantages over the multi-layer perceptron (MLP) of short training time. The RBFNN consists of three layers: an input layer, a hidden layer, and an output layer. The hidden layer contains a number of RBF neurons; each of them represents a single radial basis function, with associated centre and width. The most popular RBF is a Gaussian type that is characterized by a centre (C_j), and a positive scalar called width (r_j), where $\emptyset_j(x)$ is the output of the nonlinear activation function in the hidden layer. It is given by a Gaussian basis function as follows:

$$\varphi_j(x, c, r) = \exp[-(\frac{\|x - c_j\|}{r_j})^2] \quad , j = 1,\ldots n_h$$

Where(x) is the input vector and (n_h) is the number of nodes in the hidden layer. The network outputs are computed as a linear weighted sum of the hidden node outputs:

$$y_k(x) = \sum_j w_{kj} \quad \varphi_j(x) + b_k$$

Where (w) is the weight of the (j^{th}) centre, and (Ø) is some radial function.

B. Input-Output Determination of RBF Model

The first step towards developing a neural network model of the process is to obtain training data. Training data is obtained by designing a set of random amplitude signals (RAS) for the five inputs to the reactor: monomer feed rate, fouling factor, ambient temperature, impurity factor ,and valve position, as shown in Fig.2. These five inputs are the system inputs (monomer feed rate, manipulated variable) included the uncertainties and disturbances in the process. The second step towards developing a neural network model of the process is to determine the network input variables and the input vector and output vector. The network input vector consists of the past values of the five system inputs and the past values of the three system outputs. The determination of the inputs and outputs of the system is based on the equations (1) to (5). A total data set of 2000 samples is collected from the system Simulink model, and 4s are used as the sampling time. The first 1500 samples are used for training the network model, and the remaining 500 samples are used for testing the network model. Before training and testing, the raw data is scaled linearly into the range of [0 1] using the following formulae:

$$u = \begin{bmatrix} m_M \\ 1/hf \\ T_{amb} \\ i \\ C \end{bmatrix}, \quad y = \begin{bmatrix} T_{jin} \\ T_{jout} \\ T \end{bmatrix}$$

$$X_{scalled}(k) = \frac{x(k) - x(i)_{min}}{x(i)_{max} - x(i)_{min}}$$

After determining and scaling the input and output vectors of the system, the non-linear autoregressive with exogenous inputs (NARX) model is used to represent the non-linear dynamics of the reactor as shown in Eq.7.

C. RBF model training data Acquisition for open-loop and Validation

In this research, an RBF network is used to represent the NARX model in Eq. (7). Thus, in order to get a good training result with minimum modelling error, several numbers of maximum lags in the outputs and inputs, and several numbers of the maximum time delay in the inputs are tried. The maximum lags in the output were selected as 3, the maximum lags in the input is selected as 2, and the maximum time delay in the inputs is selected as 2, as described in Eq. (7). Thus, the RBF model is designed to have 19 inputs and 3 outputs, as shown in Fig.6. The hidden layer nodes are selected as 21. The centres are chosen using a K-means clustering algorithm as 21. Moreover, a p-nearest-neighbours algorithm is used to choose the widths. In the training of the network model, the recursive least squares (RLS) algorithm is used to update the weight matrix since the weights are linearly related to the output, and the parameters of the RLS algorithm are selected as follows: $\mu = 0.999$ and $w(0) = 10^{-6} * U_{(nh,3)}$, $p(0) = 10^{6} * I_{(nh)}$, where μ is the forgetting factor, I is an identity matrix, U is the element unity matrix (matrix with all elements are 1), and nh is the number of hidden layer nodes.

$$x(t) = [y(t \quad 1,:) \; y(t-2,:) \; y(t-3,:) \; u(t-k-1,:)]^T \qquad (7)$$

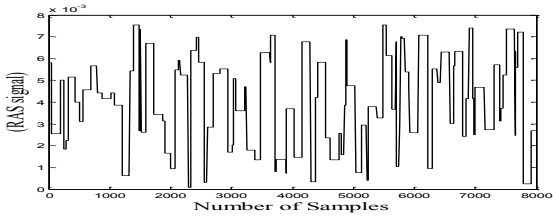

Figure 2. RAS signal.

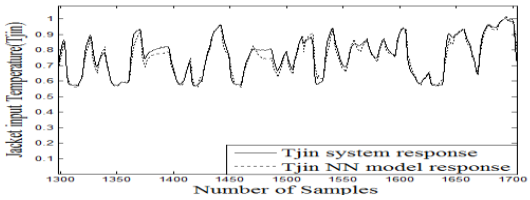

(a)

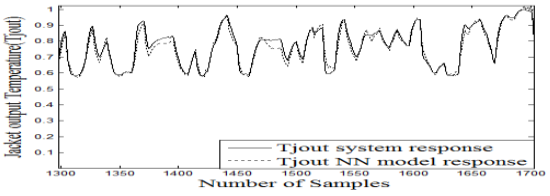

(b)

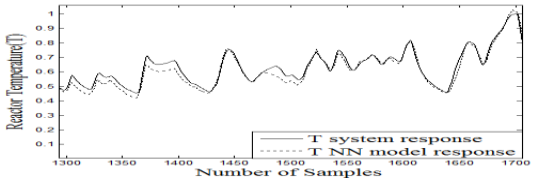

(c)

Figure 3. a,b,and c show the simulation results of jacket input temperature, jacket output temperature, and reactor temperature for system outputs and RBFNN model outputs.

Fig.3 shows the last 200 sample intervals in the training data set and the first 200 sample intervals in the testing data set. It can be clearly seen that the model outputs track the system output with a small modelling error. The mean absolute error (MAE) for the jacket input

temperature, jacket output temperature and reactor temperature are 0.004, 0.0054 and 0.0072, respectively.

IV. FAULT DETECTION

A. Simulating Faults

In this study, after training the independent RBF network model with healthy data, the model will be tested with faulty data. The faulty data is obtained by simulating different faults in the proposed reactor. These faults are classified as three sensor faults and one actuator fault. The sensor faults are jacket input temperature sensor fault, jacket output temperature sensor fault, and reactor temperature sensor fault, and the actuator fault is the inlet temperature. These faults are simulated as following:

1) Simulating Sensor Faults: The jacket input temperature sensor fault is superimposed with 10% change of the measured jacket input temperature, and simulated from the sample number 400 to 500, as shown in Fig.4. Additionally, the jacket output temperature sensor fault is superimposed with 10% change of the measured jacket output temperature, and simulated from the sample number 600 to 700, as shown in Fig.4. Furthermore, the sensor fault of the reactor temperature is superimposed with 10% change of the measured temperature, and simulated from the sample number 800 to 900, as shown in Fig.4.

2) Simulating Actuator Fault: The heating-cooling function is influenced by an equal-percentage valve with valve position. When the valve position $c < 50\%$, cooling water with inlet temperature (278.71 k) is inserted into the cooling jacket. When the valve position $c > 50\%$, steam with temperature (449.82 k) is injected into the recirculating water stream, which will lead to heating up of the coolant. Consequently, it is assumed here that a failure in the pump position of cooling mode has occurred, which leads to increase in the temperature by 10% change of the measured inlet temperature. This inlet temperature fault is simulated from the sample number 1000 to 1100, as shown in Fig.4.

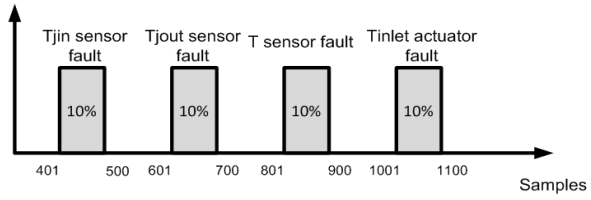

Figure 4. Fault structure with respect to number of samples.

B. Simulation results

Fig.6 demonstrates the fault detection approach. An independent model is implemented in parallel with the system to generate the residuals for detecting the sensor and actuator faults in the reactor. After training the network model with healthy random data, as described in the previous section, all four faults were simulated to the reactor model. Then, with another set of 2000 samples, faulty square data is collected. These faulty data are collected by designing a set of square waves for all inputs. These five inputs are the system inputs (monomer feed rate, manipulated variable) included the uncertainties and disturbances in the process. The second step towards developing a neural network model of the process is to determine the network input variables and the input vector and output vector. The network input vector consists of the past values of the five system inputs and the past values of the three system outputs. Where the (mM) , $(\frac{1}{h_f})$, (T_{amb}), (i) and $c(t)$ are the inputs of the system; and jacket input temperature(T_{jin}) , jacket output temperature (T_{jout}) and reactor temperature (T) are the outputs of the system. Moreover, the collected data is scaled linearly. After determining and scaling the input and output vectors of the system, the multivariable NARX is used to represent the non-linear dynamics of the reactor, The maximum lags in the output were selected as 3, the maximum lags in the input is selected as 2, and the maximum time delay in the inputs is selected as 2, as described in Eq. (8). Here again the neural network is realised by a RBF network with Gaussian basis functions. Moreover, the centres are chosen again using a K-means clustering algorithm and the widths are chosen using p-nearest-neighbours. Different numbers of hidden nodes, such as 21, 31, and 51, are used in order to get good results. The recursive least squares algorithm is used to update the weight matrix. The parameters of the recursive least algorithm are selected as follows: the forgetting factor$\mu = 0.99$, $w(0) = 1 * 10^{-5} * \mathrm{ones}(nh, 5)$, $p(0) = 1 * 10^{5} * I(nh)$.The RBF network model is tested with these faulty square data to generate fault–detection residuals. The filtered model prediction errors are shown in Fig.5. The first model prediction error of jacket input temperature is shown in Fig.5 (a), and that for jacket output temperature and reactor temperature are shown in Fig.5 (b) and Fig.5 (c), respectively. In this study, the residual ε is generated as the sum-squared filtered modelling error as follows:

$$e(k) = [y(k) - \hat{y}(k)]$$

$$\varepsilon(k) = \sqrt{e^2_{Tjin} + e^2_{Tjout} + e^2_{T}}$$

The residuals of testing the neural model are slightly bigger than the residuals of training the neural model. The mean absolute error (MAE) index is used to evaluate the modelling effects. The MAE for the jacket input temperature, jacket output temperature and reactor temperature are 0.004, 0.0054and 0.0072, respectively. Fig.10 demonstrates the residuals after using a low pass filter. It can be observed that the independent network model output is not influenced by any type of fault, because an independent model does not use past faulty measurements as inputs. Thus, it can be clearly noticed that all faults have been clearly detected. Moreover, no false alarms are thereby produced, so this verifies that the proposed scheme has shown excellent diagnostic performance.

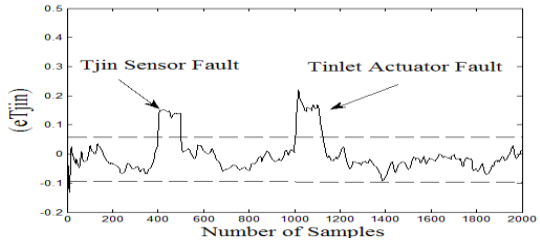

(a)

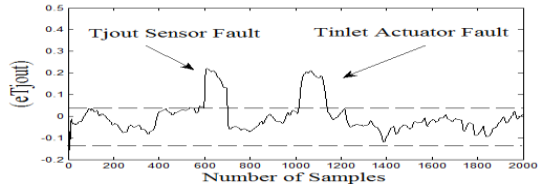

(b)

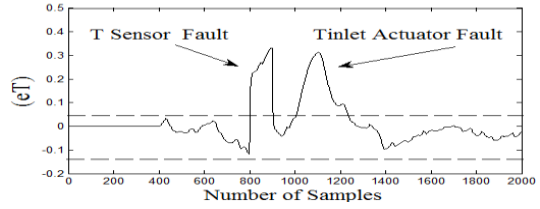

(c)

Figure 5. (a), (b), and (c) show residual filtered model prediction errors of T_{jout} , T_{jin} and T.

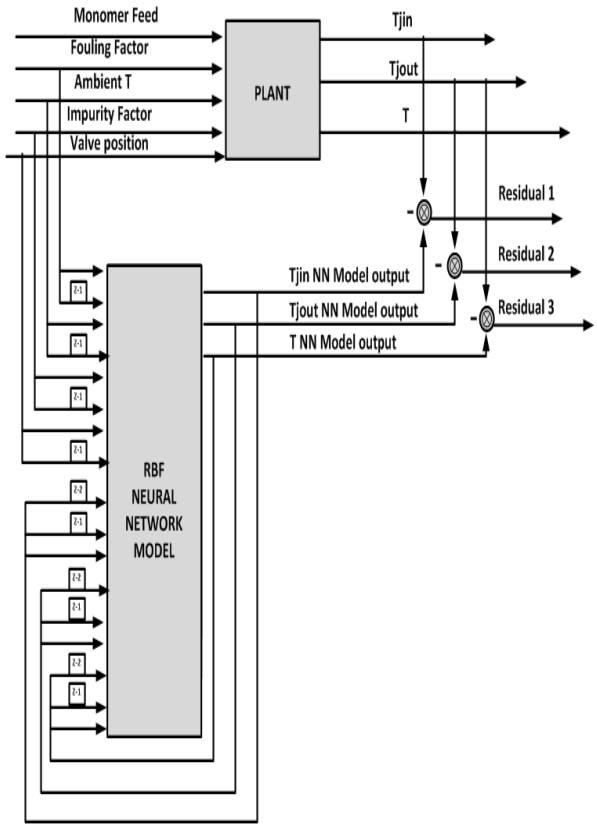

Figure 6. The structure of FD using an independent RBFNN.

V. FAULT ISOLATION

Fault isolation is the determination of the kind, location and time of detection of a fault. Fig.7 illustrates the fault isolation strategy; an additional neural network is applied as a classifier for fault isolation. The application of NNs for fault isolation has been used by many researchers, such as Patton et al.(1994) and Yu et al.(1999) used an RBF network, Yu et al.(1996a) using an MLP network, and Patton and Benkhedda (1996) used a B-spline network. In the fault detection, a residual is generated to report a fault occurring. However, it is difficult to identify which fault has occurred among all pre-specified possible faults using the residual, due to the fact that the residual is a scalar and carries little information about fault types. In this work, it is proposed to isolate faults according to model prediction errors. The model prediction errors are multi-dimensional, three-dimension in this case, and different faults will have different impacts on these vectors in three-dimension vector space. Classification of these features of different faults on the model prediction error vectors will lead to classification of different faults. Therefore, the faults that have occurred can be isolated. In this work, the neural classifier is developed by an RBF network with Gaussian basis functions. The residuals that shown in Fig.5.which are the difference between the real system output and the tested neural output were used as inputs for RBF network classifier. Moreover, the neural classifier was developed with five outputs, with four outputs associated to the four faults, and one output for (no-fault) case. The centres are chosen again using a K-means clustering algorithm and the widths are chosen using p-nearest-neighbours. Different numbers of hidden nodes, such as 51, 151, and251, are used in order to get good results. Finally 51 hidden layer nodes are selected and the centres are chosen as 51. The parameters of the recursive least algorithm are selected as follows: the forgetting factor $\mu = 0.999$, $w(0) = 1 * 10^{-5} * \mathrm{rand}(\mathrm{nh}, 5)$, $p(0) = 1 * 10^{5} * \mathrm{I}(\mathrm{nh})$. The samples arranged for fault occurrence are illustrated in Table I. Moreover, the target is set such that all four outputs are set as zero for the healthy condition data, and one output is set as 1 for a specific fault, with the others remaining at zero. Thus, once the first output is 1 and the other outputs are zero, this means that the jacket input temperature sensor fault with 10% change has occurred. In the same way, the jacket output temperature sensor fault with 10% is believed to have occurred when the second output is 1, while the others remain at zero. Similarly, the reactor temperature sensor fault and the inlet temperature actuator fault with 10% changes will have occurred when the third and the forth outputs are 1. After training, the RBF network classifier is tested with another set of faulty data with the same arrangement of training data. The samples arranged for fault occurrence can be different from those of the training data. Table I shows the classification of faults with respect to the number of samples. The four outputs of the neural classifier after use of a filter are displayed in Fig.12. It can be clearly noticed that all faults have been clearly detected and isolated.

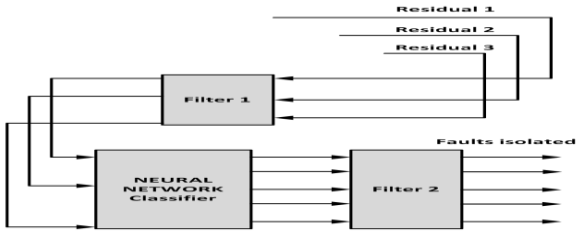

Figure 7. Block diagram for fault isolation.

TABLE I CLASSIFICATION OF FAULTS WITH RESPECT TO NUMBER OF SAMPLES

Faults	Number of samples
No fault	0~400
T_{jin} sensor fault	401~400
No fault	501~600
T_{jout} sensor fault	601~700
No fault	701~800
Reactor temperature sensor fault	801~900
No fault	901~1000
Inlet temperature actuator fault	1001~1100
No fault	1101~2000

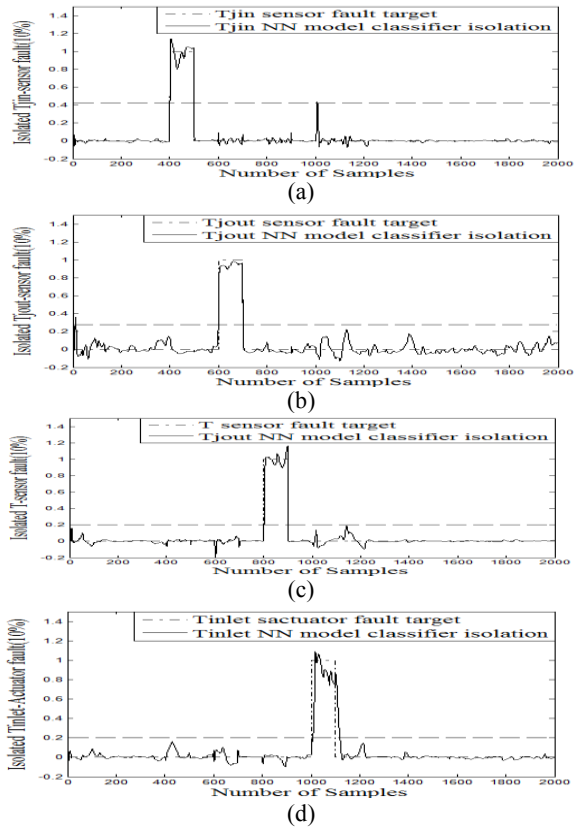

Figure 8. a, b, c, and d show the fault isolation and location for the four faults.

VI. CONCLUSION

A new robust fault diagnosis scheme has been developed for open-loop Chylla-Haase reactor using an independent radial basis function (RBF) neural network. Two different methods to employ RBF neural networks for fault diagnosis have been investigated. Three sensor faults and one actuator fault have been simulated on the Chylla-Haase reactor superimposed with 10% changes of the measured temperatures, and simulated for different numbers of samples. Moreover, the uncertainties and disturbances in the process, such as fouling factor, impurity factor, and measurement noise, have been simulated. Firstly, an independent neural network has been developed for residual generation, which is the output prediction error between a neural network and a non-linear dynamic process. Moreover, the generated residuals have been used for detecting faults. Secondly, an additional RBF neural network classifier has been developed to perform the classification task for fault isolation.

REFERENCES

[1] R.Isermann, "Process fault detection based on modelling and estimation method- a survey", Automatica, Vol.20, No.4, pp.387-404, 1984.

[2] J.Gertler, "Survey of model-based failure detection and isolation in complex plants", Control System Magazine, IEEE, Vol.8, No.6, pp.3-11, 1988.

[3] R.Delbert, R.Isermann, "Examples for fault detection in closed loops", Annual Review in Automatic Programming, Vol.17, pp.235-240, 1992.

[4] D.L.Yu, J.B.Gomm, D.Williams, "Sensor fault diagnosis in a chemical process via RBF neural networks", Control Engineering Practice, Vol.7, N.1, pp.49-55, 1999.

[5] J.B.Gomm, D.L.Yu, "Selecting radial basis function network centres with recursive orthogonal least squares training" ,IEEE Transactions on Neural Networks,Vol.11,No.2, pp.306-314, 2000.

[6] P. M. Frank, B. Koppen-Seliger, "Fuzzy logic and neural network applications to fault diagnosis", International Journal of Approximate Reasoning, Vol.16, No.1, pp.67-88, 1997.

[7] R. Chylla, D. Haase, "Temperature control of semi-batch polymerization reactors", Computers and Chemical Engineering, Vol.17, No.3, pp.257-264, 1993.

[8] M. Beyer, W. Grote, G. Reining, "Adaptive exact linearization control of batch polymerization reactors using a sigma-point kalman filter", Journal of Process Control, Vol8,No.7-8, pp.663-675, 2008.

[9] R. J. Patton, J. Chen, T. M. Siew, "Fault diagnosis in nonlinear dynamic systems via neural networks", International Conference on Control, Vol.2, pp.1346-1351, 1994.

[10] Riccardo M.G. Ferrari, Thomas Parisini, Marios M.Polycarpou, "A Robust Detection and Isolation Scheme for a Class of uncertain Input Output Discrete-time Nonlinear systems", IEEE,American Control Conference, pp.2804-2809, 2008.

[11] Xiaodong Zhang, "Sensor BiasFault Detection and Isolation in a Class of Nonlinear Uncertain systems using Adaptive Estimation", IEEE Transactions on Automatic Control, Vol.56, No.5, pp.1220-1226, 2011.